

1/f noise in MgO double-barrier magnetic tunnel junctions

G. Q. Yu,^{1,2} Z. Diao,¹ J. F. Feng,^{1,a)} H. Kurt,¹ X. F. Han,² and J. M. D. Coey¹

¹CRANN and School of Physics, Trinity College, Dublin 2, Ireland

²Beijing National Laboratory for Condensed Matter Physics, Institute of Physics, Chinese Academy of Sciences, 100190 Beijing, People's Republic of China

(Received 25 January 2011; accepted 16 February 2011; published online 16 March 2011)

Low frequency noise has been investigated in MgO double-barrier magnetic tunnel junctions (DMTJs) with tunneling magnetoresistance (TMR) ratios up to 250% at room temperature. The noise shows a $1/f$ frequency spectrum and the minimum of the noise magnitude parameter is $1.2 \times 10^{-10} \mu\text{m}^2$ in the parallel state for DMTJs annealed at 375 °C. The bias dependence of noise and TMR suggests that DMTJs with MgO barriers can be useful for magnetic field sensor applications. © 2011 American Institute of Physics. [doi:10.1063/1.3562951]

The large tunneling magnetoresistance (TMR) in MgO barrier magnetic tunnel junctions (MTJ) has greatly improved the performance of spintronic devices, such as magnetic random access memories (MRAMs), sensors, and logic devices.¹⁻⁹ The record room temperature TMR of 604% is found in single-barrier MTJs (SMTJs) with a pseudo spin valve stack,⁶ which is close to the theoretical maximum.^{1,2} However, the TMR ratio in an MTJ falls off with increasing bias.¹⁰ Double barrier MTJs (DMTJs) offer TMR of 105%—212% at room temperature¹⁰⁻¹³ but bias dependence of TMR is reduced because the applied voltage is divided over two single barriers. This helps to preserve the high TMR ratio at high bias.¹⁰ A high bias is needed to inject a sufficiently large critical current to facilitate spin transfer torque (STT) switching in magnetic nanopillars with MgO barriers, which is the basis for high-speed non-volatile STT-MRAM.¹⁴

In conventional DMTJs with a thick free layer, TMR is often lower than that in SMTJs.¹⁰⁻¹³ However, a DMTJ can potentially improve the signal-to-noise ratio of a magnetic field sensor due to the increase in output voltage compared to an SMTJ. Hence, the low frequency noise of DMTJs is worth exploring, in comparison with that of SMTJs. It has been previously reported that $1/f$ noise dominates the low frequency response of MTJs.¹⁵⁻²³ The $1/f$ noise can be characterized by a noise magnitude parameter $\alpha = AfS_V/V^2$, where A is the junction area, f is the frequency, S_V is the noise power spectrum density, and V is the applied bias.¹⁵ Recently, Guerrero *et al.*²⁴ suggested that $1/f$ noise can be greatly reduced in field sensors, when a large number of MTJs are connected either in series or in parallel. However, devices constructed with a large number of MTJs may lack integrity and suffer from a much higher chance of failure. DMTJs may be able to halve the $1/f$ noise without these drawbacks, opening up a way to reduce the noise.

Until now, a few reports have been published on the low frequency noise in DMTJs with a thick free layer^{12,20} but their TMR ratio of around 80%—120% is considerably less than we report here. Earlier studies of MgO DMTJs did not produce high TMR because the middle CoFeB layer remains amorphous after annealing.^{10-12,20} The adjacent MgO barriers cannot absorb boron, which maintains the amorphous nature of CoFeB.²⁵ Here we investigate the low frequency noise in

DMTJs, with TMR ratios as high as 222% for symmetric MgO layers and 250% for asymmetric MgO layers at room temperature. Both types of DMTJs have a similar noise level in the parallel state, and in the following we only focus on the DMTJs with symmetric MgO layers. We achieved the high TMR through the use of Co₅₀Fe₅₀ or Co₅₀Fe₅₀/Co₄₀Fe₄₀B₂₀ as free layer with high temperature postannealing, which was recently reported to improve the TMR ratio in DMTJs.¹³ We also discuss the probability of applying DMTJs as magnetic field sensors, based on their noise characteristics.

The DMTJ stacks were deposited on thermally oxidized silicon wafers at room temperature. The layer sequence was Ta 5/Ru 30/Ta 5/Ni₈₁Fe₁₉ 5/Ir₂₂Mn₇₈ 10/Co₉₀Fe₁₀ 2.5/Ru 0.9/Co₄₀Fe₄₀B₂₀(CoFeB)3/MgO 2.5/Co₅₀Fe₅₀(CoFe) t_1 /CoFeB t_2 /MgO 2.5/CoFeB 3/Ru 0.9/Co₉₀Fe₁₀ 2.5/Ir₂₂Mn₇₈ 10/Ni₈₁Fe₁₉ 5/Ta 5/Ru 5 (thickness in nanometers). When the thickness of the free layer is ≤ 2.5 nm, only CoFe t_1 is used while a CoFe 2/CoFeB t_2 bilayer is adopted for thicknesses > 2.5 nm. Moreover, DMTJs have also been grown with asymmetric MgO layers having $t_1 + t_2 = 3$ nm. The highest TMR is found when $t_1 = 2$ nm. For a comparative experiment, SMTJs consisting of Ta 5/Ru 30/Ta 5/Ni₈₁Fe₁₉ 5/Ir₂₂Mn₇₈ 10/Co₉₀Fe₁₀ 2.5/Ru 0.9/CoFeB 3/MgO 2.5/CoFeB 3/Ta 5/Ru 5 were also grown. The metallic layers of the MTJs were grown by dc sputtering and the MgO layers were grown by rf-sputtering using our Sharmrock cluster deposition tool. All MTJs were fabricated by UV lithography and Ar ion milling with junction sizes of 20×20 — $50 \times 150 \mu\text{m}^2$. High vacuum postannealing was performed in the temperature range of 250–375 °C in an applied magnetic field of 800 mT for 1 h. The magnetotransport and noise measurements are conducted as described in our previous publication.²² Positive bias represents electron flow from top to bottom CoFeB layers.

Figure 1 shows the resistance-area product (RA) versus magnetic field of a DMTJ with the CoFe 2 nm/CoFeB 0.8 nm free layer at $T_a = 375$ °C. H_{ex1} and H_{ex2} denote the exchange bias of the lower and upper reference layers. The three steps in the RA- $\mu_0 H$ curve correspond to the magnetization reversals of the free layer and two reference layers. Also shown is the normalized low frequency noise power spectrum integrated across an octave centered at 4.8 Hz as a

^{a)}Electronic mail: jfeng@tcd.ie.

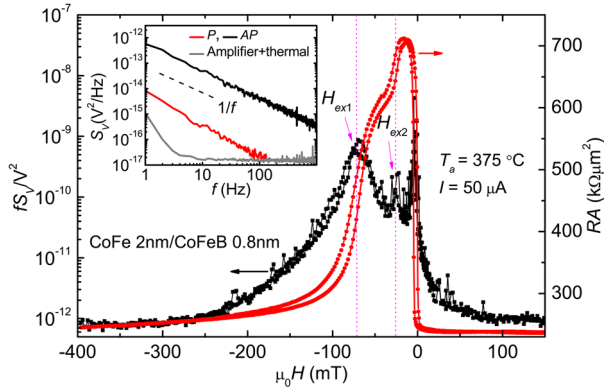


FIG. 1. (Color online) The magnetic field dependence of the normalized $1/f$ noise in an octave centered at 4.8 Hz and the RA- H curve for a DMTJ with the middle free layer CoFe 2 nm/CoFeB 0.8 nm, annealed at $T_a=375^\circ\text{C}$. Inset shows the noise power spectral density as a function of frequency in the P and AP states after subtracting the thermal and amplifier noise.

function of field for the same DMTJ. The noise peaks coincide with switching of the ferromagnetic layers. By applying a sufficiently large field (≥ 60 mT), the magnetic fluctuations can be suppressed. The remaining noise power is mainly attributed to the barrier noise, which is independent of field. Here we apply magnetic fields of 60 and -20 mT to set the parallel (P) and antiparallel (AP) states in the DMTJ, and measure the noise spectra up to 1 kHz. A $1/f$ spectrum is observed in both cases (Fig. 1 inset), with the AP state being much noisier than the P state.^{15–17,19–21}

Figure 2(a) shows the T_a dependence of α in the P state (α_p) for representative DMTJs and SMTJs. The α_p value decreases with T_a for both types, which reflects a gradual improvement of the interfaces between the ferromagnetic layers and the MgO tunnel barrier. When T_a exceeds 350°C , α_p becomes stable due to the fact that CoFeB layers are fully crystallized at the MgO/CoFeB interfaces. The lowest α_p value in SMTJs is $1.8 \times 10^{-10} \mu\text{m}^2$ at $T_a=375^\circ\text{C}$, which is similar to that reported in Refs. 19–21. The lowest α_p in DMTJs is $1.2 \times 10^{-10} \mu\text{m}^2$, as shown in Fig. 3(a). The α_p in DMTJs is not half of that in corresponding SMTJs, as would otherwise be expected from connecting two MTJs in series. This can be attributed to the fact that the two tunnel barriers

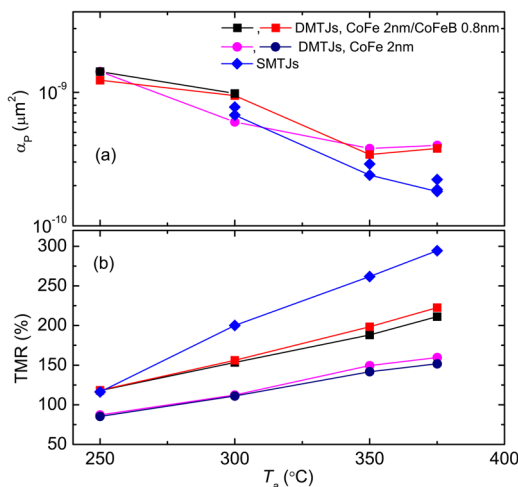


FIG. 2. (Color online) The annealing temperature dependence of the noise magnitude parameter (α) in the P state (a) and the corresponding TMR (b) for selected SMTJs and DMTJs with symmetric MgO layers.

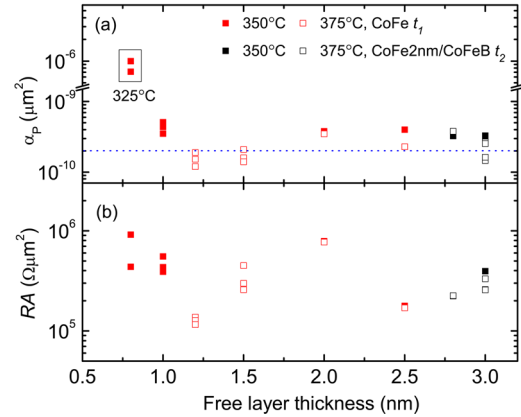


FIG. 3. (Color online) (a) The noise magnitude parameter (α) in the P state and (b) the corresponding RA values as a function of the thickness of the middle free layer in DMTJs with symmetric MgO layers. The line in (a) indicates the minimum noise level reported in Ref. 21.

are not exactly the same, with the upper barrier suffering a less ideal growth condition compared to the lower one. Hence, the noise characteristics of these DMTJs may be dominated by the upper MgO barriers.

We find no direct correlation between noise and the TMR ratio in both SMTJs and DMTJs. In the low T_a range, TMR also increases rapidly with T_a [Fig. 2(b)], which is due to the improved interfaces as mentioned above. For the 3 nm free layer, the highest TMR values obtained at room temperature after annealing at $T_a=375^\circ\text{C}$ are 295% in SMTJs, 222% in DMTJs with symmetric MgO layers, and 250% in DMTJs with dissimilar MgO layers. Compared to DMTJs with only 2 nm CoFe as the free layer, we find that inserting a thin amorphous CoFeB layer can effectively increase the TMR ratio. This is due to a more ideal growth condition for (001)-oriented MgO on top of the CoFeB. After annealing, B in the thin CoFeB is absorbed by the CoFe layer while keeping its bcc crystalline phase, because B cannot diffuse into the high quality MgO barriers.²⁵

The noise magnitude parameter α_p in DMTJs as a function of the thickness of the middle free layer is shown in Fig. 3(a). All noise measurements were made with a bias in the range of 10–30 mV. No random telegraph noise is seen. The highest $\alpha_p \approx 10^{-6} \mu\text{m}^2$ is measured when t_1 is 0.8 nm. This may indicate that the 0.8 nm CoFe layer is discontinuous and it greatly degrades the MgO barrier grown on top. However, when the thickness of the free layer is ≥ 1.0 nm, α_p is at least three orders of magnitude lower, reaching $10^{-10} \mu\text{m}^2$. α_p varies with the thickness of the free layer in these DMTJs. The lowest α_p in the range of $1.2\text{--}2.1 \times 10^{-10} \mu\text{m}^2$ is found for $t_1=1.2\text{--}1.5$ nm. Interestingly, the RA values of these DMTJs also vary in a roughly similar manner with the thickness of the free layer. The lowest RA also appears around $t_1=1.2$ nm [see Fig. 3(b)]. Further experiments are required to investigate this correlation in detail.

It is known that the voltages for which the TMR value is reduced to half of its maximum ($\pm V_{1/2}$) are higher for DMTJs than for SMTJs.¹⁰ As shown in Fig. 4(a), the values of $\pm V_{1/2}$ in TMR are $+1.1$ and -1.1 V for a DMTJ while they are $+0.66$ and -0.62 V for an SMTJ, respectively. Here we use α in the AP state (α_{AP}) to elucidate its bias dependence. We find that there is a sharper reduction in noise with bias compared to that in TMR. The values of $\pm V_{1/2}$ for α_{AP} are

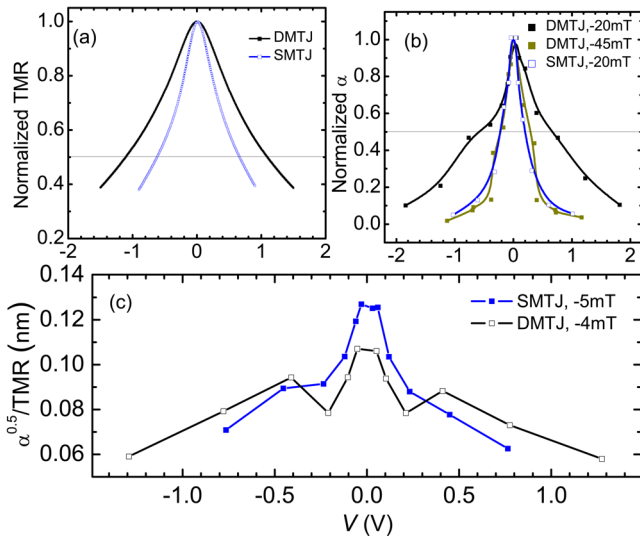


FIG. 4. (Color online) The bias dependence of (a) TMR, (b) the noise magnitude parameter in the antiparallel state and (c) the $\alpha^{0.5}/\text{TMR}$ value during free layer switching for an SMTJ and a DMTJ with symmetric MgO layers. The lines in (b) are guides to the eye.

around +0.74 and -0.65 V for the same DMTJ while they are around +0.34 and -0.22 V for the corresponding SMTJ. In contrast to the bias dependence of TMR, α_{AP} in DMTJs and SMTJs varies asymmetrically with bias, reflecting dissimilar CoFeB/MgO interfaces in the MTJ stacks^{11,13} and possibly more oxygen vacancies appearing at the top interfaces.²² Importantly, $V_{1/2}$ in both α and TMR for DMTJs is approximately double that for SMTJs.^{10,12} The noise-bias dependence was also measured for the DMTJ at -45 mT, where only the magnetization of the bottom pinned CoFeB layer switches. The α value at -45 mT has a very similar variation with bias compared to that for SMTJs [Fig. 4(b)]. This further confirms that DMTJs behave in a way similar to two SMTJs connected in series. However, more complex behavior than sequential tunneling might be considered, as reported in a previous work.²⁶

Only the free layer is manipulated around zero field in magnetic field sensors. To show the possibility of DMTJs as field sensors, the noise during the magnetization reversal of the middle free layer is also measured; see Fig. 4(c). $1/f$ noise is again observed. It is found that TMR decreases slowly while the noise of middle free layer decreases fast with bias in DMTJs. Figure 4(c) shows the $\alpha^{0.5}/\text{TMR}$ value as a function of bias for a DMTJ and an SMTJ. If the device is perfectly linearized, this $\alpha^{0.5}/\text{TMR}$ is proportional to the field detection capability in different types of MTJs.^{8,12} It is found that $\alpha^{0.5}/\text{TMR}$ in the DMTJ is lower than that in the corresponding SMTJ under low bias but the two curves cross each other at +0.32 and -0.36 V. The field detection capability is enhanced with bias, for both SMTJs and DMTJs, as previously reported by Almeida *et al.*¹² For low bias operation, our results suggest that these DMTJs may offer a better field detection capability compared to SMTJs.

In conclusion, comparison of low frequency noise in DMTJs and SMTJs with high TMR ratios shows that the noise magnitude parameter in DMTJs is slightly lower, close to $1 \times 10^{-10} \mu\text{m}^2$ in the P state. Like the TMR, the noise in

the AP state for DMTJs decays slowly with bias compared to that for SMTJs. Bias dependence of both α and TMR suggests these DMTJs behave like two SMTJs in series, with no sign of coherent/resonant tunneling. DMTJs can be useful for magnetic field sensors, and may offer a better signal to noise ratio compared to SMTJs under low bias.

This work was supported by SFI as part of the MANSE Project No. 2005/IN/1850, and was conducted under the framework of the INSPIRE program, funded by the Irish Government's Programme for Research in Third Level Institutions, Cycle 4, National Development Plan 2007–2013. This work was also supported by the Ireland-China exchange agreement.

¹W. H. Butler, X.-G. Zhang, T. C. Schulthess, and J. M. MacLaren, *Phys. Rev. B* **63**, 054416 (2001).

²J. Mathon and A. Umersky, *Phys. Rev. B* **63**, 220403 (2001).

³S. Yuasa, A. Fukushima, T. Nagahama, K. Ando, and Y. Suzuki, *Nature Mater.* **3**, 868 (2004).

⁴S. S. Parkin, C. Kaiser, A. Panchula, P. M. Rice, B. Hughes, M. Samant, and S. H. Yang, *Nature Mater.* **3**, 862 (2004).

⁵D. D. Djayaprawira, K. Tsunekawa, M. Nagai, H. Maehara, S. Yamagata, N. Watanabe, S. Yuasa, Y. Suzuki, and K. Ando, *Appl. Phys. Lett.* **86**, 092502 (2005).

⁶S. Ikeda, J. Hayakawa, Y. Ashizawa, Y. M. Lee, K. Miura, H. Hasegawa, M. Tsunoda, F. Matsukura, and H. Ohno, *Appl. Phys. Lett.* **93**, 082508 (2008).

⁷G. Reiss and D. Meyners, *J. Phys.: Condens. Matter* **19**, 165220 (2007).

⁸P. P. Freitas, R. Ferreira, S. Cardoso, and F. Cardoso, *J. Phys.: Condens. Matter* **19**, 165221 (2007).

⁹T. Kawahara, R. Takemura, K. Miura, J. Hayakawa, S. Ikeda, Y. M. Lee, R. Sasaki, Y. Goto, K. Ito, T. Meguro, F. Matsukura, H. Takahashi, H. Matsuoka, and H. Ohno, *IEEE J. Solid-State Circuits* **43**, 109 (2008).

¹⁰G. Feng, S. van Dijken, and J. M. D. Coey, *Appl. Phys. Lett.* **89**, 162501 (2006).

¹¹T. Nozaki, A. Hirohata, N. Tezuka, S. Sugimoto, and K. Inomata, *Appl. Phys. Lett.* **86**, 082501 (2005).

¹²J. M. Almeida, P. Wisniewski, and P. P. Freitas, *J. Appl. Phys.* **103**, 07E922 (2008).

¹³H. D. Gan, S. Ikeda, W. Shiga, J. Hayakawa, K. Miura, H. Yamamoto, H. Hasegawa, F. Matsukura, T. Ohkubo, K. Hono, and H. Ohno, *Appl. Phys. Lett.* **96**, 192507 (2010).

¹⁴J. A. Katine and E. E. Fullerton, *J. Magn. Magn. Mater.* **320**, 1217 (2008).

¹⁵E. R. Nowak, M. B. Weissman, and S. S. P. Parkin, *Appl. Phys. Lett.* **74**, 600 (1999).

¹⁶L. Jiang, E. R. Nowak, P. E. Scott, J. Johnson, J. M. Slaughter, J. J. Sun, and R. W. Dave, *Phys. Rev. B* **69**, 054407 (2004).

¹⁷C. Ren, X. Y. Liu, B. D. Schrag, and G. Xiao, *Phys. Rev. B* **69**, 104405 (2004).

¹⁸D. Mazumdar, X. Y. Liu, B. D. Schrag, M. Carter, W. F. Shen, and G. Xiao, *Appl. Phys. Lett.* **91**, 033507 (2007).

¹⁹J. Scola, H. Polovy, C. Fermon, M. Pannetier-Lecoq, G. Feng, K. Fahy, and J. M. D. Coey, *Appl. Phys. Lett.* **90**, 252501 (2007).

²⁰J. M. Almeida, P. Wisniewski, and P. P. Freitas, *IEEE Trans. Magn.* **44**, 2569 (2008).

²¹R. Stearrett, W. G. Wang, L. R. Shah, A. Gokce, J. Q. Xiao, and E. R. Nowak, *J. Appl. Phys.* **107**, 064502 (2010).

²²Z. Diao, J. F. Feng, H. Kurt, G. Feng, and J. M. D. Coey, *Appl. Phys. Lett.* **96**, 202506 (2010).

²³R. Stearrett, W. G. Wang, L. R. Shah, J. Q. Xiao, and E. R. Nowak, *Appl. Phys. Lett.* **97**, 243502 (2010).

²⁴R. Guerrero, M. Pannetier-Lecoq, C. Fermon, S. Cardoso, R. Ferreira, and P. P. Freitas, *J. Appl. Phys.* **105**, 113922 (2009).

²⁵H. Kurt, K. Rode, K. Oguz, M. Boese, C. C. Faulkner, and J. M. D. Coey, *Appl. Phys. Lett.* **96**, 262501 (2010).

²⁶F. Montaigne, J. Nassar, A. Vaurès, F. Nguyen Van Dau, F. Petroff, A. Achuhl, and A. Fert, *Appl. Phys. Lett.* **73**, 2829 (1998).